Nov 5th, 12:00 AM - 12:00 AM

Numerical Studies of Rivet-Fastened Rectangular Hollow Flange Channel Beams

R. Siahaan

P. Keerthan

M. Mahendran

Twenty-Second International Specialty Conference on Cold-Formed Steel Structures
St. Louis, Missouri, USA, November 5 & 6, 2014

Numerical Studies of Rivet-Fastened Rectangular Hollow Flange Channel Beams

R. Siahaan[1], P. Keerthan[2] and M. Mahendran[3]

Abstract:

The rivet-fastened rectangular hollow flange channel beam (RHFCB) is a new cold-formed hollow section proposed as an alternative to welded hollow flange beams. It is a monosymmetric channel section made by rivet-fastening two torsionally rigid rectangular hollow flanges to a web plate. This method will allow the designers to develop optimum sections, with affordable rivet connection between their web and flange elements. In addition to this unique geometry, the rivet-fastened RHFCBs also have unique characteristics relating to their stress-strain characteristics, residual stresses, initial geometric imperfections and hollow flanges that are not encountered in conventional hot-rolled and cold-formed steel channel sections. Therefore detailed experimental and numerical studies were conducted to study the section moment capacities of rivet-fastened RHFCBs. This paper presents the details of the numerical study of rivet-fastened RHFCBs and the results. Finite element models of rivet-fastened RHFCBs were developed by including all the significant effects that influence their ultimate section moment capacities, including material inelasticity, and geometric imperfections. The results from finite element analyses were then compared with corresponding experimental results and the predictions from the current design rules. Test results showed that the developed finite element models were able to predict the behaviour and section moment capacities of RHFCBs. The validated model was then used in a detailed parametric study that produced additional section moment capacity data of the rivet-fastened RHFCBs.

Keywords: *Rivet-Fastened Rectangular Hollow Flange Channel Beams, Cold-formed Steel Beams, Section Moment Capacity, Direct Strength Method, and Finite Element Analyses.*

[1]PhD Researcher, [2]VC Research Fellow, [3]Professor, Science and Engineering Faculty, Queensland University of Technology, Australia.

1.0 Introduction

The use of cold-formed steel members in buildings has increased considerably due to the availability of advanced manufacturing technology. Although cold-formed steel members are considered to be more cost-efficient than hot-rolled steel members, they suffer from complex buckling modes. For instance, the more common C and Z sections are more susceptible to distortional buckling. Hence advanced cold-formed, hollow flange sections (HFS) were introduced: first the Dogbone section and later the LiteSteel Beam. They were widely used as flexural members in residential, industrial & commercial buildings. However, both sections have been recently discontinued due to the expensive dual electric resistance welding process used in manufacturing, as well as other factors.

The rivet-fastened RHFCB (Figure 1) has much more affordable rivet-fastening connection between its flange and web elements, as well as the flexibility of using different combinations of flange and web steel thicknesses and grades due to the way that is it being assembled. It also has additional lips, possibly contributing to additional strength.

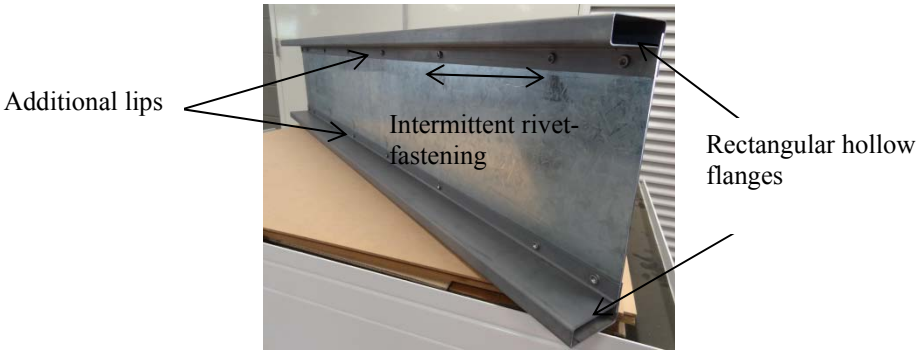

Figure 1: Rivet-Fastened Rectangular Hollow Flange Channel Beam

Much research has been carried out on LSB sections including the shear capacity (Keerthan and Mahendran 2011; Keerthan et.al 2014), section moment capacity (Anapayan et al. 2011a; Anapayan and Mahendran 2012), lateral distortional buckling (Anapayan et al. 2011b) as well as capacities of LSBs with web openings (Seo and Mahendran 2011,2012). However, the flexural behaviour and strength of the rivet-fastened RHFCB is not known and the effect of rivet-fastening is not accounted for in the currently available design provisions. Recent experimental studies have shown the existence of inelastic

reserve bending capacity on cold-formed steel beams (Anapayan et al. 2011a, Shifferaw and Schafer 2012). The Australian cold-formed design standard (AS/NZS 4600), which is similar to the North American Cold-Formed Steel Specification, allows for the inclusion of inelastic reserve capacity but cannot be used for hollow flange steel beams as they do not meet two of the conditions outlined in Clause 3.3.2.3. Further research is therefore needed.

The primary design method used for cold-formed steel members is the effective width method. The Direct Strength Method (DSM) was developed as an alternative, more simplified method, for determining the strength of cold-formed steel members. The DSM uses elastic buckling moment which can be easily obtained from computer software such as THIN-WALL or CUFSM, combined with first yield moment, to determine the strength of a member. Over the years, significant work related to DSM has been completed. Yu and Schafer (2007) found that DSM yields reasonable strength predictions for local and distortional buckling failures of C and Z section beams with a wide range of industry standard geometries and yield stresses of steel between 228 to 506 MPa. Shifferaw and Schafer (2012) proposed design methods for inelastic local, distortional, and lateral-torsional buckling that were integrated into the existing DSM in the 2012 Edition of the North American Specification. As the current AS/NZS 4600 and AS 4100 design standards do not have suitable provisions for the effect of rivet-fastening, this study aims to investigate the suitability of the DSM in computing the section moment capacity of rivet-fastened RHFCBs.

An experimental study was first carried out to investigate the section moment capacity of rivet-fastened RHFCB subject to local buckling effects. This was followed by a numerical study to develop validated finite element models of rivet-fastened RHFCBs. Accurate validation of the finite element model and its subsequent use allowed the extension of test data of RHFCBs with varying section geometry, grade of steel and rivet spacing. This paper presents the details of the numerical study including the development of finite element model, its validation and the parametric study, and the results.

2.0 Experimental Studies

Fifteen section moment capacity tests were conducted to study the flexural behaviour of rivet-fastened RHFCBs subject to local buckling effects. Initially, the experimental study was aimed at investigating the behaviour of RHFCB sections with different compactness: compact, non-compact, and slender. However, due to manufacturing limitations, only slender sections could be manufactured and tested.

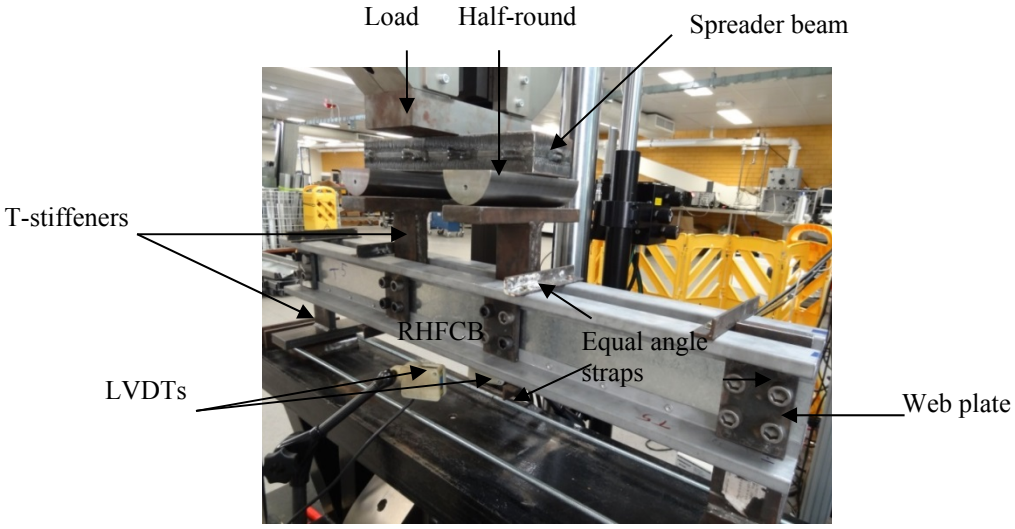

Figure 2: Laboratory Test Set-Up

Table 1: Ultimate Section Moment Capacities of Rivet-Fastened RHFCBs from FEA and Tests

Test No.	Rivet Spacing (mm)	RHFCB Sections d x b_f x d_f x t_f x t_w, (mm)	Test M_u (kNm)	FEA M_u (kNm)	Test/FEA
1	100	152x62x19x1.1x1.9	7.97	8.4	0.95
2		201x62x19x1.1x1.9	12.08	11.04	1.09
3		250x62x19x1.1x1.9	14.88	13.84	1.08
4		150x53x18x0.9*x1.4	5.32	-	-
5		150x53x18x1.1x1.4	6.40	6.96	0.92
6		201x53x18x0.9*x1.9	9.46	-	-
7		201x53x18x1.1x1.9	11.36	10.44	1.09
8		250x62x19x0.9*x1.9	11.98	-	-
9		250x62x19x1.1x1.4	12.24	13.72	0.89
10	50	152x62x19x1.1x1.9	8.45	9.88	0.86
11		201x62x19x1.1x1.9	13.03	14.32	0.91
12		250x62x19x1.1x1.9	16.27	17.56	0.93
13	200	152x62x19x1.1x1.9	6.92	7.12	0.97
14		201x62x19x1.1x1.9	10.30	9.52	1.08
15		250x62x19x1.1x1.9	12.76	12.16	1.05

Note: d-depth, b_f-flange width, d_f-flange depth, t_f-flange thickness, t_w-web thickness, M_u- ultimate moment. * Yield stress of 0.9 mm sheet is unavailable.

The section moment capacity tests were conducted using back to back RHFCB specimens to prevent twisting. A four point bending arrangement was used to simulate the critical central region of uniform bending moment. Figure 2 shows the test set-up where all the tested beams have the same length of 1200 mm. A suitable arrangement was selected to eliminate any shear buckling failures.

The two, back to back, RHFCB specimens were connected with 10 mm thick web plate and T-shaped stiffeners at the loading and support locations using four M16 bolts. T-shaped stiffeners were used to support and transfer the loads to the web elements of test beams and thus avoided web crippling failures. Lateral buckling was prevented by using four angle straps on the compression flanges and two straps on the tension flanges to tie the beams together as shown in Figure 2. The use of straps to provide lateral restraint in a back to back section moment capacity test had previously been adopted by other researchers (Pham and Hancock 2013). An LVDT was placed underneath each beam specimen in the uniform bending moment region to measure the vertical deflection at md-span. The applied load and vertical deflections at mid-span were measured until post-failure. Table 1 presents the results from tests and finite element analyses.

3.0 Finite Element Modelling

3.1 General

A detailed finite element (FE) model was developed to study the flexural behaviour and capacity of rivet-fastened RHFCB subject local buckling effects. This section describes the developed FE model. The FE model in this study was developed using MSC/Patran pre-processing facilities and then submitted to ABAQUS for analysis. The results were then viewed using MSC/Patran as post-processing facilities. The presence of symmetry permitted the modelling of only half of the span while the cross-section geometry of the FE model was based on the measured dimensions given in Table 1, and using centreline dimensions. This is because shell elements that were used for the RHFCB model in this study discretise a body by defining the geometry at the reference surface (the centreline of the body). Also, t_w and t_f in Table 1 refer to the base metal thicknesses measured after removing coating. In the FE model, rounded corners of RHFCBs were omitted as their effect was considered small.

The FE simulation in this study consists of two steps: bifurcation buckling and non-linear static analysis. Bifurcation buckling analyses were used to obtain eigenvectors for the inclusion of geometric imperfections where an imperfection

magnitude of web depth/150 was used. The lowest Eigenvalue was selected as it is usually the critical mode and was then used in the nonlinear static analysis to define the shape and distribution of initial geometric imperfections.

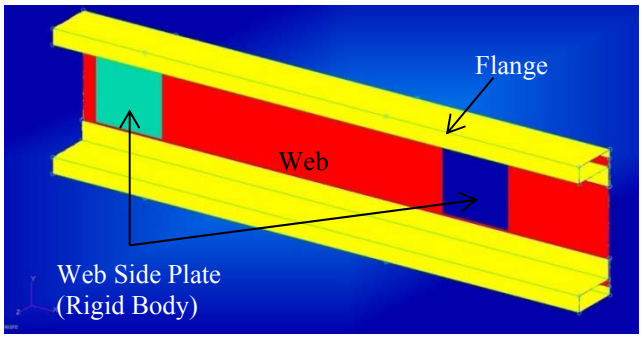

Figure 3: Geometry of Rivet-Fastened RHFCBs with Web Side Plates

3.2 Finite Element Mesh

The ABAQUS S4R5 element was selected in all the finite element models. This element is a thin, shear flexible, isoparametric quadrilateral shell with four nodes and five degrees of freedom per node, utilising reduced integration and bilinear interpolation schemes. R3D4 rigid body elements were used to simulate the web side plates used in the tests. The R3D4 element is a rigid quadrilateral with four nodes and three translational degrees of freedom per node. Convergence studies showed that an element size of 5 mm x 5 mm provided an accurate representation of the flexural behaviour of RHFCBs. The geometry of a typical rivet-fastened RHFCB with web stiffener plates is shown in Figure 3 while Figure 4 shows typical finite element mesh used in RHFCB models.

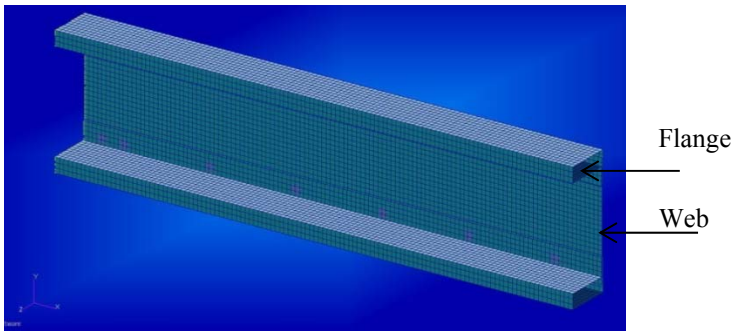

Figure 4: Typical Finite Element Mesh for Rivet-Fastened RHFCBs

3.3 Material Model and Properties

The ABAQUS classical metal plasticity model was used in all the analyses. This model implements the von Mises yield surface to define isotropic yielding, associated plastic flow theory, and either perfect plasticity or isotropic hardening behaviour. A perfect plasticity model was adopted in all the finite element models. Measured yield stresses were used in the analyses. The elastic modulus and Poisson's ratio values were taken as 200,000 MPa and 0.3, respectively.

3.4 Loads and Boundary Conditions

The presence of symmetry permitted the modelling of only half of the span. Although the rivet-fastened RHFCBs were tested back to back, only one of the beams was simulated. Simply supported end conditions were used in the model.

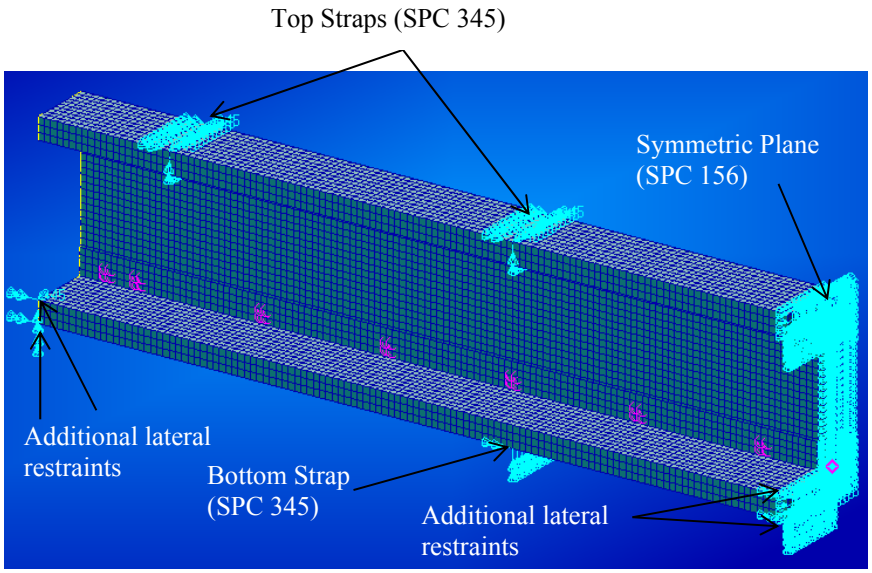

Figure 5: Boundary Conditions at Strap Location and Symmetry Plane

In the experiments, lateral restraint was provided by equal angle straps at the top and bottom flanges. During the experiments, no strap failure was observed. Therefore, based on this observation, the straps were not explicitly modelled. Instead, they were simulated using boundary condition as follows (Figure 5):

$$u_x = 0\ u_y = 0\ u_z = 1\ \theta_x = 1\ \theta_y = 1\ \theta_z = 0$$

In the above, u_x, u_y and u_z denote translations and θ_x, θ_y and θ_z denote rotations in the x, y and z directions, respectively, and "0" denotes free while "1" denotes restrained. Additional lateral restraints were included at four points on the bottom flange to eliminate any lateral displacement and twisting of the bottom flange. Since only half of the beam was modeled, the following boundary condition was applied to simulate cross-section symmetry (Figure 5):

$$u_x = 1\ u_y = 0\ u_z = 0\ \theta_x = 0\ \theta_y = 1\ \theta_z = 1$$

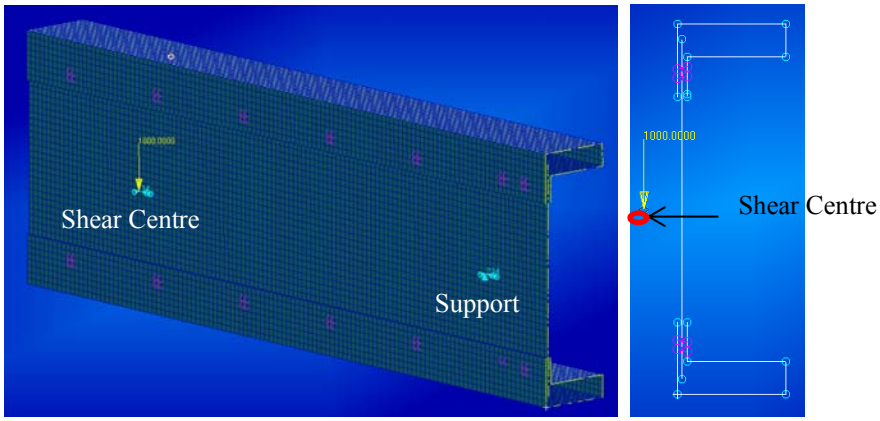

Figure 6: Boundary Conditions at Support and Loading Point

Support boundary conditions:

$$u_x = 0\ u_y = 1\ u_z = 1\ \theta_x = 1\ \theta_y = 0\ \theta_z = 0$$

Shear centre loading was used in this study to prevent twisting of beam where the location of the shear centre was obtained by modelling the section in THIN-WALL. Theoretically, shear centre varies where the rivet connection is and between rivets (no connection between web and lips). However, as the load was transferred from T-stiffeners and web plate, shear centre at the rivet connection can be used. Figure 6 shows the location of the shear centre of a typical rivet-fastened RHFCB with a 1000 N applied load. At the loading point, the following boundary condition is applied:

$$u_x = 0\ u_y = 0\ u_z = 1\ \theta_x = 1\ \theta_y = 0\ \theta_z = 0$$

The laboratory test set-up included 75 mm wide web stiffeners plates at each support and loading point to prevent lateral movement and twisting of the cross

–section. These stiffening plates were modelled as rigid bodies using R3D4 elements. Simply supported boundary conditions were applied to the rigid body reference node at the shear centre in order to provide ideal pinned supports.

3.5 Initial Geometric Imperfections and Residual Stresses

The magnitude of local imperfections was taken as web depth/150 for all the rivet-fastened RHFCB specimens. The critical imperfection shape was introduced using the *IMPERFECTION option in ABAQUS. In this analysis, the effects of residual stresses were neglected. Since the rivet-fastened RHFCBs do not undergo welding process, they do not have membrane residual stresses. Further, the effect of flexural residual stresses due to cold-forming is assumed to be negligible as there is beneficial strength increase in the corner region.

3.6 Rivet Modelling

Rivets play an important role in the flexural behaviour of rivet fastened RHFCBs. This study assumed that rivet failure is unlikely to occur as confirmed by our experiments. Hence rivet fasteners connecting web and flange elements were not explicitly modelled. Instead, they were simulated using Tie MPCs, which make all active degrees of freedom equal on both sides of the connection. The web side plates at the supports were connected using high strength steel bolts (M16 8.8/S) to avoid bolt failures during testing. Our bending tests confirmed that there were no bolt or plate failures. Therefore these web side plates were modelled as rigid bodies using R3D4 elements. In this study, the connection between the lips and web was modeled as contacts. Here lips were defined as the master surfaces and the web was defined the slave surface.

3.7 Analysis Methods

In this study, two methods of analysis were used, namely elastic buckling analysis and nonlinear static analysis. Elastic buckling analysis is focused on determining the buckling mode of the section. Although elastic buckling is not a direct predictor of capacity or collapse behaviour, both the mode and the buckling moment from this analysis are important parameters that affect the actual behaviour of the beam. The buckling loads from elastic buckling are often used as parameter for predicting strength in design specifications such as in the case of DSM while the buckling shape is used for the input of imperfection when its maximum amplitude is known but its distribution is not known. Nonlinear static analyses, including the effects of large deformations and material yielding, were used to investigate the flexural behaviour of rivet fastened RHFCBs until failure. The RIKS method in ABAQUS was also

included in the nonlinear analyses. Following parameters were used in the non-linear analyses: Maximum number of load increments = 100, Initial increment size = 0.01, Minimum increment size = 0.000001, Automatic increment reduction enabled, and large displacements enabled.

4.0 Validation of Finite Element Model

It is necessary to validate the developed finite element models of rivet-fastened RHFCBs subject to local buckling effects. 13 finite element models were developed and Table 1 presents a summary of the FEA results of ultimate section moment capacities and a comparison with corresponding test results. The mean and COV of the ratio of test to FEA moments are 0.98 and 0.088, respectively. This indicates that the finite element models developed in this study are able to predict the ultimate moment capacities of rivet-fastened RHFCBs reasonably well. Figure 7 shows the failure modes of 201x62x19x1.1 x1.9 RHFCB rivet-fastened at 200 mm (Test Specimen 14). Figure 8 shows the failure modes from FEA and experiment, respectively for 150x53x18x1.1x1.4 RHFCB rivet-fastened at 100 mm spacing (Test Specimen 5).

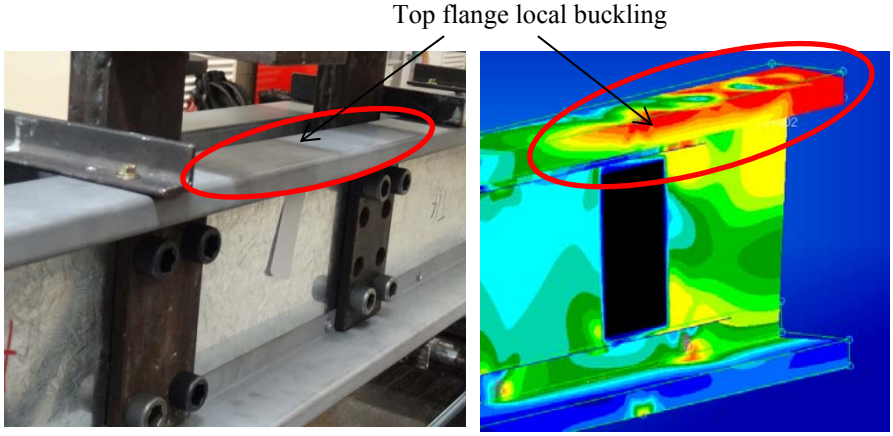

(a) Test (b) FEA

Figure 7: Failure Mode of 201x62x19x1.1x1.9 RHFCB Rivet-Fastened at 200 mm spacing

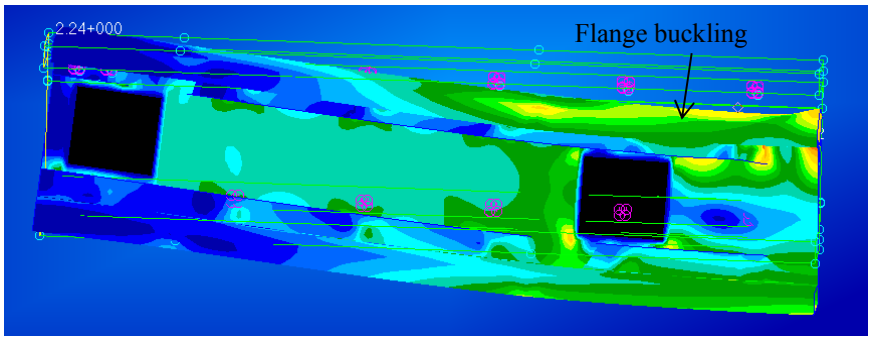

(a) FEA

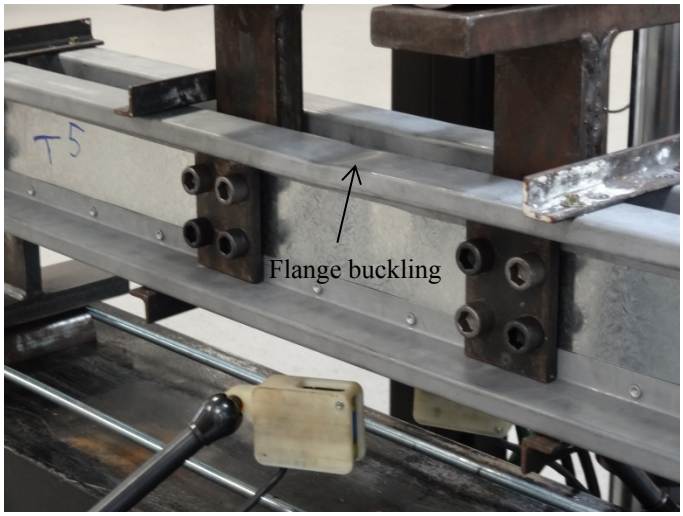

(b) Experiments

Figure 8: Failure Mode from FEA and Experiment of 150x53x18x1.1x1.4 RHFCB Rivet-Fastened at 100 mm spacing

Figure 9 shows a typical applied moment versus deflection graphs of rivet-fastened RHFCBs from FEA and experiments. Although the ultimate moments agree well, there is a difference between the load-deflection graphs. Apart from slip that happens in the early stages of tests, it is believed that this is due to variations/errors in the measurement of small deflections and the locations where they were measured. In summary, a reasonably good agreement between the results from FEA and experiments in terms of ultimate moments, failure modes and moment versus deflection graphs confirm the adequacy of the

developed finite element models of rivet-fastened RHFCBs. However, research is continuing to improve the FE models further in relation to their ability to simulate the effect of contact surfaces between web and flanges more accurately.

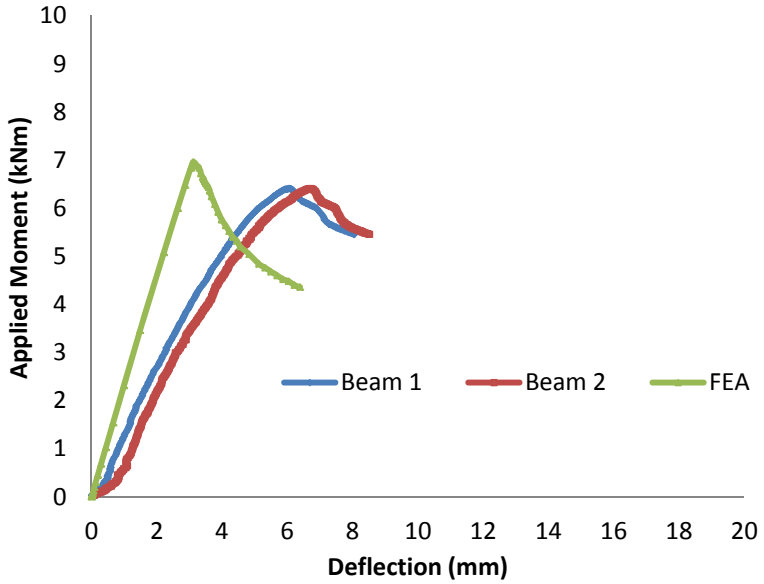

Figure 9: Plot of Applied Moment versus Deflection for Test Specimen 5

5.0 Comparison with Current Design Rules

The section moment capacities (M_s) of all the 15 tested rivet-fastened RHFCBs were calculated based on the design method in AS/NZS 4600, which is identical to the North American Specification (AISI S100). They were also calculated using the Australian hot-rolled design standard (AS 4100) for comparison purposes. Table 3 shows the ratios of the ultimate moments (M_u) from FEA and tests to the section moment capacities (M_s) calculated using both standards.

From the results in Table 3, AS/NZS 4600 appears to better predict the section moment capacities of rivet-fastened RHFCBs. Note that the M_s values for the RHFCBs with different rivet spacings (50, 100 and 200 mm) are the same as both design standards do not have any provision for the effect of rivet fastening. Therefore this study aims to explore the suitability of the DSM to predict the section moment capacity of rivet-fastened RHFCBs as described next.

Table 3: Comparison of Ultimate Moment Capacities of RHFCBs with AS/NZS 4600 and AS 4100 Predictions

Test No.	Rivet Spac -ing	RHFCB Sections ($d \times b_f \times d_f \times t_f \times t_w$)	AS/NZS 4600			AS 4100		
			M_s (kNm)	M_u/M_s		M_s (kNm)	M_u/M_s	
				Test	FEA		Test	FEA
1	100	152x62x19x1.1x1.9	7.16	1.11	1.17	5.82	1.37	1.44
2		201x62x19x1.1x1.9	11.03	1.10	1.00	8.86	1.36	1.25
3		250x62x19x1.1x1.9	15.50	0.96	0.89	12.27	1.21	1.13
4		150x53x18x0.9*x1.4	-	-	-	-	-	-
5		150x53x18x1.1x1.4	6.46	0.99	1.08	5.96	1.07	1.17
6		201x53x18x0.9*x1.9	-	-	-	-	-	-
7		201x53x18x1.1x1.9	10.69	1.06	0.98	9.65	1.18	1.08
8		250x62x19x0.9*x1.9	-	-	-	-	-	-
9		250x62x19x1.1x1.4	14.20	0.86	0.97	12.60	0.97	1.09
10	50	152x62x19x1.1x1.9	7.16	1.18	1.38	5.82	1.45	1.70
11		201x62x19x1.1x1.9	11.03	1.18	1.30	8.86	1.47	1.62
12		250x62x19x1.1x1.9	15.50	1.05	1.13	12.27	1.33	1.43
13	200	152x62x19x1.1x1.9	7.16	0.97	0.99	5.82	1.19	1.22
14		201x62x19x1.1x1.9	11.03	0.93	0.86	8.86	1.16	1.07
15		250x62x19x1.1x1.9	15.50	0.82	0.78	12.27	1.04	0.99

Note: M_u = Ultimate moment, M_s = Section moment capacity. * Yield stress data is unavailable for 0.9 mm beams. M_u from Test and FEA are listed in Table 1.

6.0 Parametric Study and Proposed Design Equations

Following the validation of the developed FE models, a detailed parametric study was undertaken based on the validated FE models to develop suitable design rules for rivet-fastened RHFCBs subject to bending actions. 21 rivet-fastened RHFCB models were analysed using nominal section dimensions and mechanical properties. Table 4 shows the FEA and test results of 15 rivet-fastened RHFCBs in DSM format while Table 5 shows the parametric study results of 100 mm rivet-fastened RHFCBs. In the parametric study, 100 mm rivet spacing was chosen as it is considered to be more practical for adoption. However, in our future work, other rivet spacings will also be modeled. In the parametric study, some of the sections that were tested as part of the experimental study were re-modelled with different flange and web yield stresses. New compact and non-compact sections with thicker flanges and web elements were also modelled in order to include all three types of sections (i.e. compact, non-compact and slender) in the DSM plot. For the purposes of DSM plot, section slenderness parameter λ, equal to the square root of the ratio of first yield moment (M_y) and elastic buckling moment from FEA(M_{ol}) was calculated.

Table 4: Section Moment Capacities of Rivet-Fastened RHFCBs (DSM Format)

Test No.	Rivet Spacing (mm)	RHFCB Sections d x b_f x d_f x t_f x t_w (mm)	M_{ol} (kNm)	$\lambda = \sqrt{\frac{M_y}{M_{ol}}}$	M_u/M_y	
					Test	FEA
1	100	152x62x19x1.1x1.9	7.19	1.16	0.83	0.87
2		201x62x19x1.1x1.9	9.87	1.22	0.82	0.75
3		250x62x19x1.1x1.9	12.92	1.25	0.73	0.68
4		150x53x18x0.9*x1.4	-	-	-	-
5		150x53x18x1.1x1.4	6.84	1.11	0.77	0.83
6		201x53x18x0.9*x1.9	-	-	-	
7		201x53x18x1.1x1.9	9.94	1.17	0.84	0.77
8		250x62x19x0.9*x1.9	-	-	-	-
9		250x62x19x1.1x1.4	9.94	1.45	0.59	0.66
10	50	152x62x19x1.1x1.9	9.57	1.00	0.88	1.03
11		201x62x19x1.1x1.9	14.87	0.99	0.89	0.97
12		250x62x19x1.1x1.9	20.96	0.98	0.80	0.87
13	200	152x62x19x1.1x1.9	6.29	1.24	0.72	0.74
14		201x62x19x1.1x1.9	8.74	1.29	0.70	0.65
15		250x62x19x1.1x1.9	11.53	1.33	0.63	0.60

Table 5: Parametric Study Results of RHFCBs Rivet-Fastened at 100 mm

RHFCB Sections	Yield stress (MPa)		OC	M_{ol} (kNm)	M_y (kNm)	M_u (kNm)	λ	M_u/M_y
	Flange	Web						
150x53x18x1.1x1.4	250	500	S	6.84	5.65	5.44	0.91	0.96
150x53x18x1.1x1.4	450	500	S	6.84	10.17	7.92	1.22	0.78
150x53x18x1.1x1.4	500	500	S	6.84	11.31	8.48	1.29	0.75
150x53x18x1.1x1.4	550	500	S	6.84	12.44	9.12	1.35	0.73
201x53x18x1.1x1.9	300	300	S	9.94	10.99	9.44	1.05	0.86
201x53x18x1.1x1.9	450	450	S	9.94	16.49	12.12	1.29	0.74
250x62x19x1.1x1.4	250	250	S	9.94	14.08	10.52	1.19	0.75
250x62x19x1.1x1.4	300	300	S	9.94	16.89	11.92	1.30	0.71
250x62x19x1.1x1.9	300	300	S	12.92	16.44	12.64	1.13	0.77
250x62x19x1.1x1.9	450	300	S	12.92	24.66	15.28	1.38	0.62
250x62x19x1.1x1.9	500	300	S	12.92	27.41	14.64	1.46	0.59
250x62x19x1.1x1.9	550	300	S	12.92	30.15	15.64	1.53	0.56
125x45x15x2.0x2.0	250	250	C	35.40	7.09	8.48	0.45	1.20
125x45x15x2.0x2.0	300	300	C	35.40	8.51	9.92	0.49	1.17
125x45x15x2.0x2.0	450	380	C	35.40	12.76	13.96	0.60	1.09
200x60x20x2.0x2.0	250	250	C	38.27	16.51	16.16	0.66	0.98
200x60x20x2.0x2.0	300	300	NC	38.27	19.81	18.84	0.72	0.95
200x60x20x2.0x2.0	450	450	NC	38.27	29.72	26.56	0.88	0.89
200x60x20x2.5x2.5	300	300	C	71.36	24.64	27.16	0.59	1.10
200x60x20x2.5x2.5	380	350	C	71.36	31.21	31.08	0.66	1.00
200x60x20x2.5x2.5	450	380	C	71.36	36.96	33.52	0.72	0.91

* Yield stress for 0.9 mm sheet is unavailable; OC denotes overall compactness.

7.0 Direct Strength Method

The Direct Strength method (DSM) is an alternative procedure for determining the strength of cold-formed steel members. It uses elastic buckling moment (M_{ol}) which can be easily obtained from finite strip software such as CUFSM and THIN-WALL, or from finite element analysis. Hence the DSM can be used to predict the section moment capacity of RHFCBs as elastic buckling moments can be calculated from FEA for varying rivet-spacings. Since AS 4100 is a standard for hot-rolled steel and the AS/NZS 4600 does not have any provision for rivet spacing, it is of interest to investigate the suitability of the DSM to predict the moment capacities of rivet-fastened RHFCBs. However, the DSM based design rules are based on research work on conventional C and Z sections.

DSM design rules for local buckling

The nominal section moment capacity (M_s) is determined from Section 1.2.2.1.2.1.1 (Equation 1.2.2-8) of AISI-S100 as follows:

$$M_s = \left(\left(1 - 0.15\left(\frac{M_{ol}}{M_y}\right)^{0.4}\right)\left(\frac{M_{ol}}{M_y}\right)^{0.4}\right) M_y \quad (1)$$

where: M_s = section moment capacity, M_{ol} = elastic buckling moment, M_y= first yield moment, $\lambda = \sqrt{M_y/M_{ol}}$. Therefore:

$$\frac{M_s}{M_y} = \frac{1}{\lambda^{0.8}} - \frac{0.15}{\lambda^{1.6}} \quad (2)$$

As for the inelastic region, the section moment capacity (M_s) for sections symmetric about the axis of bending or sections with first yield in compression is determined from Section 1.2.2.1.2.1.2 (Equation 1.2.2-10) in AISI-S100 by Equation 3.

$$M_s = M_y + (1 - \frac{1}{C_{yl}{}^2})(M_p - M_y) \quad (3)$$

where: M_p=plastic moment, $C_{yl} = \sqrt{0.776/\lambda} \leq 3$, $\lambda = \sqrt{M_y/M_{ol}}$.

Section 4 demonstrated the accuracy of the developed FE model of rivet-fastened RHFCBs. In the proposed design method based on DSM, M_{ol} can be obtained from FEA of rivet-fastened RHFCBs and thus it can predict M_s accurately for RHFCBs with varying rivet spacings. Figure 10 compares the FEA and test results based on Tables 4 and 5 with DSM design equations in a

non-dimensional plot of M_s/M_y versus $\lambda=\sqrt{(M_y/M_{ol})}$. This figure shows that the DSM based equations (1) and (3) predict the section moment capacities of rivet-fastened RHFCBs reasonably. This comparison also includes the inelastic moment capacity region. Figure 10 also includes the section moment capacity test results of continuously welded hollow flange channel beams, LSBs.

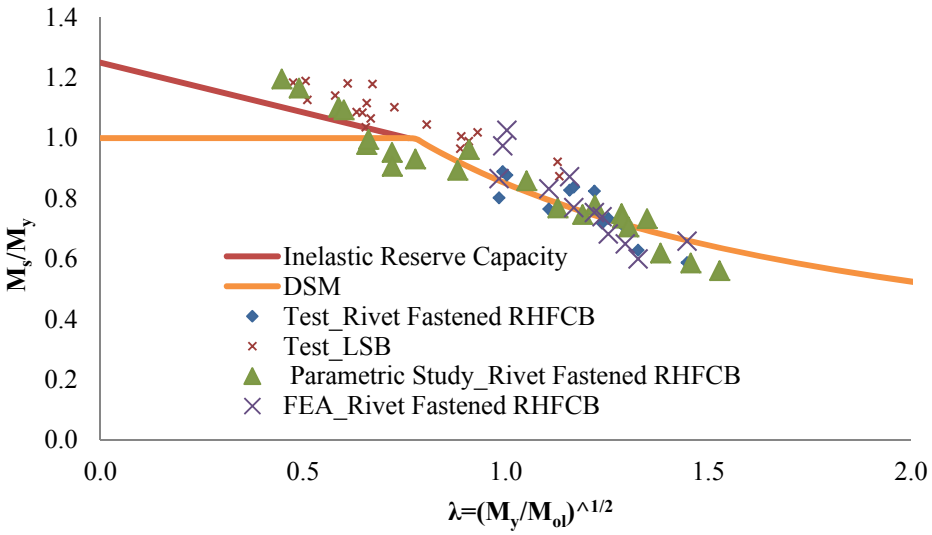

Figure 10. Direct Strength Method based Design

8.0 Conclusions

This paper has presented a detailed investigation into the section moment capacity of rivet-fastened RHFCBs using finite element analyses. Suitable finite element models were developed and validated by comparing their results with corresponding test results. The developed nonlinear finite element model was able to predict the section moment capacities of rivet-fastened RHFCBs and associated deformations and failure modes with a reasonably good accuracy. However, research is continuing to further refine the finite element model.

Comparison of ultimate moment capacities from finite element analysis and test results with design capacity predictions from the current cold-formed and hot-rolled steel structures design standards showed that the cold-formed steel structures design standard was able to better predict the section moment

capacities of rivet-fastened RHFCBs as long as the rivet spacing was small. At present, there is no provision to predict the effect of rivet-fastening in currently available standards and consequent capacity reduction as rivet spacing increases. However, the DSM based design rules can be used to include the effects of rivet spacing. It was found that the current DSM based design rules are able to predict the section moment capacities of rivet-fastened RHFCBs reasonably well. Further studies are continuing to develop accurate DSM equations for rivet fastened RHFCBs.

Acknowledgements

The authors would like to thank Queensland University of Technology for providing a Vice-Chancellor's research fellowship and a postgraduate scholarship and the necessary facilities and support to conduct this research project.

REFERENCES

American Iron and Steel Institute (AISI S100) (2012), "North American Specification for the Design of Cold-Formed Steel Structural Members", Washington, D.C., USA.

Anapayan, T., Mahendran, M. and D. Mahaarachchi. (2011a). "Section Moment Capacity Tests of LiteSteel beams." Thin-Walled Structures 49(4): 502-512.

Anapayan, T., Mahendran, M. and D. Mahaarachchi. (2011b). "Lateral Distortional Buckling Tests of a New Hollow Flange Channel Beam." Thin-Walled Structures 49(1): 13-25.

Anapayan, T. and M. Mahendran (2012). "Numerical Modelling and Design of LiteSteel Beams Subject to Lateral Buckling." Journal of Constructional Steel Research 70(0): 51-64.

Keerthan, P., et al. (2014). "Experimental studies of hollow flange channel beams subject to combined bending and shear actions." Thin-Walled Structures 77(0): 129-140.

Keerthan, P. and M. Mahendran (2011). "New Design Rules for the Shear Strength of LiteSteel Beams." Journal of Constructional Steel Research 67(6): 1050-1063.

Pham, C. and G. Hancock (2013). "Experimental Investigation and Direct Strength Design of High-Strength, Complex C-Sections in Pure Bending." Journal of Structural Engineering 139(11): 1842-1852.

Seo, J. K. and M. Mahendran (2011). "Plastic bending behaviour and section moment capacities of mono-symmetric LiteSteel beams with web openings." Thin-Walled Structures 49(4): 513-522.

Seo, J. K. and M. Mahendran (2012). "Member moment capacities of mono-symmetric LiteSteel Beam floor joists with web openings." Journal of Constructional Steel Research 70(0): 153-166.

Shifferaw, Y. and B. Schafer (2012). "Inelastic Bending Capacity of Cold-Formed Steel Members." Journal of Structural Engineering 138(4): 468-480.

Standards Australia (SA 1998), AS 4100-1998, “Steel Structures”, Sydney, Australia.

Standards Australia (SA 2005), AS/NZS 4600-2005, “Cold-formed Steel Structures”, Sydney, Australia.

Yu, C. and B. W. Schafer (2007). "Simulation of Cold-formed Steel Beams in Local and Distortional Buckling with Applications to the Direct Strength Method." Journal of Constructional Steel Research 63(5): 581-590.